State selective dynamics of TiO_2 charge carrier trapping and recombination

Yu Zhang,[a,b,c] *Daniel T. Payne,*[a,b] *Chi L. Pang,*[a,b] *Cephise Cacho,*[c] *Richard T. Chapman,*[c] *Emma Springate,*[c] *Helen H. Fielding,*[a] *and Geoff Thornton*[a,b,1]

[a] Department of Chemistry, 20 Gordon Street, University College London, London WC1H 0AJ, UK

[b] London Centre for Nanotechnology, 17-19 Gordon Street, University College London, London WC1H 0AH, UK

[c] Central Laser Facility, STFC Rutherford Appleton Laboratory, Didcot OX11 0QX, UK

[1] To whom correspondence should be addressed. E-mail: g.thornton@ucl.ac.uk.

KEYWORDS

Charge carriers recombination | trapping | TiO_2 | electron dynamics | ultrafast dynamics

Abstract

Time-resolved pump-probe photoemission spectroscopy has been used to study the dynamics of charge carrier recombination and trapping on hydroxylated rutile TiO_2(110). Two types of pump excitation were employed, one in the infrared (0.95 eV) and the other in the UV (3.5 eV) region. With IR excitation, electrons associated with defects are excited into the bottom of the conduction band from the polaronic states within the band gap, which are retrapped within 45±10 fs. Under UV excitation, the electrons in these band gap state (BGS) and valence band electrons are excited into the conduction band. In addition to the fast polaron trapping observed with IR excitation, we also observe a long lifetime (about 1 ps) component to both the depletion of hot electrons at the bottom of the conduction band and the refilling of the BGS. This points to a BGS mediated recombination process with a ps lifetime.

The recombination pathways of charge carriers are of paramount importance in photocatalysis because they determine the lifetime of chemically active sites, and hence the catalytic efficiency. These pathways are not known in detail even for a prototypical material such as TiO_2, in part because of challenges associated with the presence of polaronic trapping centres[1–7]. The relationship between the associated trapping processes and the charge carrier recombination dynamics is important in a number of applications of TiO_2 in addition to photocataysis, such as its use as an electron collector in perovskite solar cells[8].

The study of the recombination dynamics in TiO_2 has so far relied on techniques such as photoluminesence and transient absorption spectroscopy (TAS) [9,10]. Both techniques have provided valuable results down to the fs regime, with TAS allowing the dynamics of electrons and holes to be examined independently. However, neither method can monitor the recombination in a state selective manner, which is achieved in this work through the use of time-resolved femtosecond pump-probe photoemission spectroscopy.

A schematic diagram of the valence band and conduction band density of states of hydroxylated rutile TiO_2 is shown in Fig.1[11]. The accepted picture of TiO_2 photocatalysis involves photoexcitation of electrons across the 3 eV band gap[12]. More recently, a second photoabsorption channel with a threshold at about 3 eV has been identified, although it is not yet clear what, if any, role it plays in photocatalysis[13–15]. This channel involves excitation from the polaronic Ti 3d BGS, which have an apparent binding energy of 0.8 eV, into a resonance in the conduction band that lies 3.5 eV above. In this study we investigate the recombination of charge carriers and electron trapping associated with the valence and conduction bands as well as the BGS. The results point to the importance of the BGS in both fast and slow decay of hot

charge carriers. BGS not only absorb photons and form transient excited states, but also trap band electrons and holes to accelerate recombination.

Experiments

Measurements were performed using the Artemis condensed matter end station at the Central Laser Facility, Rutherford Appleton Laboratory[16]. The end station consists of a SPECS Phoibos 100 hemispherical energy analyser as well as a SPECS low energy electron diffraction (LEED) and Auger electron spectroscopy (AES) instrument. The base pressure of the end station was 9×10^{-11} mbar. A reduced rutile TiO_2(110) crystal, blue in color, was cleaned by a few Ar^+ sputtering (1 kV, 1μA/cm^2, 15 min) and annealing (1100 K, 5 min) cycles. This resulted in an ordered surface showing a sharp (1×1) rutile TiO_2(110) LEED pattern, and AES confirmed its cleanliness. The surface was allowed to hydroxylate through reaction of the oxygen vacancies with water in the residual vacuum. The expected coverage of hydroxyls being approximately 10% of a monolayer (1 ML=5.22×10^{14} unit cells/cm^2) [17,18]. This surface, which is denoted h-TiO_2(110), was chosen for study because of its long term stability[19].

An s-polarised experimental geometry was employed for time resolved photoemission spectroscopy measurements (see Fig. 1) to avoid laser-assisted photoelectric effects[20]. Both pump and probe pulses are driven by a Ti:Sapphire chirped pulse amplification system (RedDragon, KMLabs, 1 kHz repetition rate). The pump pulses of 0.95 eV (1300 nm, 50 fs pulse width, IR) and 3.5 eV (350 nm, 50 fs pulse width, UV) were generated from a high-energy optical parametric amplifier (HE-TOPAS, Light Conversion Ltd). The extreme UV (XUV) probe pulse (10^8 photons/sec, 30 fs pulse width) was generated using a higher harmonic generation apparatus[16], with photon energies of 20.9 eV and 30.4 eV used for the IR and UV pumped experiments, respectively. The pump and the probe laser beams were coincident at 45˚

from the surface normal. As the pump-probe signal is very small, delay scans were typically repeated more than 2000 times, with an accumulation time of up to 12 hours, to achieve an acceptable signal to noise ratio. Photoemission spectra were recorded at normal emission (±13˚ collection angle), collecting a 5 eV binding energy window from about 4 eV below E_F to 1 eV above. This encompasses the top of the valence band, the BGS and the bottom of the conduction band. The position of E_F was identified from the Ta sample holder.

The excitation processes are shown schematically in Fig. 1. In the IR-pumped experiment, a photon energy of 0.95 eV is chosen to be close to the resonance energy, 0.8 eV, found in previous IR absorption experiments[2,21]. This energy allows BGS electrons to be excited to the bottom of the conduction band, after which they become retrapped in the polaronic BGS. The delayed probe pulse then monitors the change of the BGS and the bottom of the conduction band by photoemission in order to measure the dynamics of the retrapping process. In the second experimental scheme, a photon energy of 3.5 eV is employed as the pump. From previous band gap measurements and calculations[22,23], this energy is well above the band gap of about 3 eV, and known to match a band gap absorption in rutile TiO_2. As noted above, this energy is also associated with the excitation from the BGS to a resonance state within the conduction band[13–15], which has been interpreted differently as hydroxyl induced states[15] or higher Ti 3d states[13,14]. A comparison between the dynamics induced by IR and UV pulses allows us to separate the dynamics of polarons from that of band electrons and holes.

Results

IR-pumped experiments. Fig. 2A shows photoemission spectra of the top of the valence band, the BGS and the bottom of the conduction band. The black and red curves are the spectra measured before the arrival of pump pulses (referred to as a steady state spectrum) and at a

delay time of 25 fs, respectively. The peak at about 0.8 eV binding energy is from the BGS. The upper edge of the valence band is seen at binding energies above 3 eV. In the time-delayed spectrum (red), the introduction of the IR pump laser causes a significant decrease of the BGS peak intensity and an increase in intensity around E_F. These changes can be clearly seen in the corresponding difference spectrum in the same graph. The depletion of the BGS is indicated by the negative peak at 0.8 eV, and population of hot electrons gives rise to a positive peak at around E_F. It should be noted that the excited hot electrons should in principle lie above E_F. However, due to the instrumental broadening their distribution appears to be centered at E_F. For binding energies larger than 2 eV, there is an unexpectedly large positive increase in the difference spectrum. This is mainly attributed to a shift of the valence band caused by the relaxation of surface band bending, a phenomenon known as the surface photovoltage (SPV) effect[24]. It is commonly observed for semiconductor surfaces in pump-probe measurements and has also been observed on TiO_2[25]. In this case the (red) spectrum shifts to a slightly higher energy, giving rise to a significant positive contribution in the difference spectrum where the valence band rises. To compensate for the SPV effect we shift all the IR pumped spectra to lower binding energy. The magnitude of the shift, typically about 10 meV, is determined from the SPV shift measured at around 3 eV binding energy (Supporting information S1).

Fig. 2B shows the difference spectra calculated from the raw data (left) and SPV compensated data (right) for different delay times. Compensating for SPV has the effect of removing the positive excursions below 3 eV for all delay times. It also removes small positive excursions around E_F for delay times longer than 250 fs. The SPV compensation allows us to resolve the trapping dynamics with high accuracy. It also reveals a time dependence of the intensity between 1 and 3 eV binding energy around zero time delay, which is attributed to a change of

secondary electron background arising from the elevated electron temperature. (Supporting information S2).

The dynamics of BGS depletion and hot electron population around E_F is plotted in Fig. 2C. An exponential decay function convolved with a Gaussian was applied to fit the data. The Gaussian represents the cross correlation of the IR and XUV pulses, which was obtained from a laser-assisted photoelectric effect measurement[20]. The recovery of the depleted BGS gives an exponential time constant of 45±10 fs. The error arises mainly from the uncertainty in the value of time zero. Hot electron decay has a very similar lifetime of 48±10 fs, as expected on the basis of the trapping model shown in Fig.1 C.

UV-pumped experiments. In the UV pumped measurements, an increase of hot electrons around E_F and a decrease of electrons at the top of the valence band are expected in the difference spectra. A depletion of BGS is also expected, being associated with the excitation of electrons to an energy of about 2.7 eV above E_F in the conduction band. These electrons are expected to quickly decay back to the bottom of the conduction band (<15 fs) [26,27], joining those excited from the valence band. The population of hot electrons higher in the conduction band is found to be extremely low even at the 0 fs delay time (Supporting information S3). Hence, the spectra in Fig. 3 are terminated at about 2 eV above E_F.

In Fig. 3A, the increase of hot electrons around E_F can be unambiguously identified, but the depletion at the valence band edge is complicated by the SPV effect. Difference spectra from both IR- and UV-pumped measurements are shown for a 20 fs delay time in Fig. 3A. At binding energies greater than 3 eV the positive peak in the IR spectrum will be due solely to the SPV effect. This contrasts with the UV spectrum, where there is a clear depletion at 3.5 eV

binding energy. The difference spectra obtained by shifting the delayed spectra to correct for the SPV effect are shown in Fig. 3B. This correction makes the assumption that the difference spectra at binding energies less than 3 eV is dominated by the SPV effect (Supporting information S1). Quantitative analysis of the depletion at the valence band edge is not feasible because of uncertainty in the SPV compensation. Nevertheless, it is clear that there is a reduction at 3 eV binding energy consistent with our expectations.

Further analysis of the time dependence of the UV-pumped spectra (Fig. 3C) shows that the decay of hot electrons around E_F and the recovery of the BGS behave in a similar manner as in the IR pumped spectra. However, in contrast to the IR-pumped data, both also contain a long decay component. In fitting the recovery of the BGS to two exponential decay components, one has a lifetime of 65±20 fs while the other is of the order of ps. The corresponding values for the hot electron decay are 68±20 fs and 2±2 ps. The large error bars on the fast components include the estimation of time zero, which for the UV pumped data is obtained from the correlation spectrum of the hot electrons at 1 eV above the E_F[13,27,28]. The fitting results of the long decay component have large uncertainties due to the correction of the SPV effect. However, the ps lifetime obtained from the recovery of BGS is rather reliable as the dynamics are calculated around the BGS peak position. The SPV correction process causes almost no modification around peak maxima, where the derivative is zero.

Discussion

Retrapping of polarons. The polaron trapping time of conduction band electrons has been estimated from the period of the longitudinal optical (LO) phonon mode[29] that interacts significantly with electron transport. In rutile TiO_2, the energy of this mode is 96 meV[29,30], corresponding to a period of 43 fs. This agrees well with the trapping time observed in our IR-

pumped measurements. We can also correlate our results with measurements of anatase TiO_2, where the LO phonon energy of 100 meV is close to that in rutile[31]. For anatase, it is known from resonant inelastic X-ray spectroscopy that the electron polarons are associated with LO phonons. A similar trapping time of electrons in anatase TiO_2 is therefore expected, with a 50 fs lifetime being observed in IR TAS measurements of dye-sensitised TiO_2 thin films[32]. A comparison with the results presented here suggests that this arises from polaron trapping.

We now turn to the depletion and recovery of the BGS peak in the UV-pumped experiments. The fast component of the BGS recovery (65±20 fs) is close to that observed in the IR-pumped experiment (45±10 fs), suggesting that they arise from a similar trapping process. The slightly longer recovery time of about 20 fs in the UV-pumped experiment may be attributed to the additional decay of hot electrons from a higher energy, about 2.7 eV above the E_F, to the bottom of conduction band. Theoretical calculations have investigated this relaxation process in terms of both electron-phonon [27] and electron-electron scattering[33]. The results indicate that the excess energy of hot electrons dissipates into phonons and electron-hole excitations near the Fermi level in a few tens of fs. Since these electrons are originally from localised BGS, they have a high possibility of being retrapped into polaronic states in an additional 45±10 fs.

BGS mediated recombination. There are two potential contributions to the long component of the BGS recovery. One is due to the recombination of BGS electrons with valence band holes. This is thought to give rise to photoluminescence with a ns lifetime at about 2.2 eV, significantly smaller than the band gap of 3 eV[10]. The second contribution, which will also affect the decay of hot electrons, arises from the lifetime of band electrons at the bottom of the conduction band being extended by up to a picosecond because of the reduced scattering probability of phonons[27].

The population of hot electrons around E_F is of a similar magnitude to the decrease of BGS intensity at all delay times after UV excitation (Fig. 3 B,C). At first sight this is surprising since a dominance of hot electrons created by band-gap-excitation might be expected. There are two likely factors contributing to this apparent anomaly. Firstly, the resonance nature of the BGS to conduction band excitation. Secondly, for 3.5 eV excitation the valence band density of states accessed is not significantly higher than the BGS. This is evidenced by the spectral intensity in Fig. 3A, coupled with knowledge that the photoionisation cross sections of O 2p and Ti 3d are comparable at a photon energy of about 30 eV[34].

The charge trapping and recombination processes in TiO_2 are summarised graphically in Fig. 4. The slowest process is expected to arise from direct recombination of band electrons and holes. There are photoconductivity measurements of TiO_2 that present indirect evidence of conduction band electron recombination with valence band holes, with a recombination lifetime ranging from picoseconds to ns regime[35,36]. A ns lifetime is outside of the temporal range that our experiment can access. It has been also argued that defects can trap and annihilate carriers in the conduction and valence bands on the ps timescale[9]. Recent calculations also suggest that excess electrons in polaronic states can greatly accelerate the recombination of the electron hole pairs from ns down to a few ps[37]. Related processes in our work are shown schematically in the middle of Fig. 4 in b and c. Process c causes the depletion of BGS, while process b refills them. On the basis of the Shockley-Read-Hall model, the involvement of holes will dominate the recombination processes in an n-type semiconductor since they are the minority carrier[38]. Therefore, processes b and c are correlated but the rate of the BGS refilling will be determined by the rate of BGS electron recombination with valence band holes[38]. These two processes have been directly identified here from the long time

component of the dynamics of the hot electrons and BGS, as demonstrated in Fig. 3B for UV pumped experiments. The fastest dynamics are associated with trapping of excited electrons in the polaronic BGS. A short lifetime for the two processes involved, represented by d and e in Fig. 4, presumably arises from the localised nature of the trapping events.

In summary, we have distinguished the recombination processes on the surface of h-TiO_2(110) by measuring the dynamics of relevant states. This was made possible through the use of time resolved IR/UV-pump XUV-probe spectroscopy to measure the state-resolved dynamics. The most rapid electron dynamics are associated with re-trapping of hot electrons created by excitation of polaronic band gap electrons, which makes TiO_2 an excellent material for collecting electrons in dye sensitised and organic perovskite solar cells. On the other hand, electron trapping into polaronic BGS accelerates the recombination of band electrons and holes created by UV irradiation. Our studies highlight the importance of band gap states in the photo-catalysis and photo-chemistry of TiO_2.

ACKNOWLEDGEMENTS. This work was supported by the European Research Council Advanced Grant ENERGYSURF (GT), EPSRC (UK) (EP/D068673/1), EU COST Action CM1104, and the Royal Society (UK) through a Wolfson Research Merit Award to GT.

Author contributions

G.T. designed the project. Y.Z., D.T.P, C.L.P., C.C., R.T.C., E.S., H.H.F, G.T. were involved in the measurements. Y.Z., D.T.P., G.T. analysed the data. All authors participated in writing and discussing the data.

References

1 I. G. Austin and N. F. Mott, *Adv. Phys.*, 1969, **18**, 41–102.

2 V. N. Bogomolov, Y. A. Firsov, E. K. Kudinov and D. N. Mirlin, *Phys. Stat. Sol.*, 1969, **35**, 555–558.

3 E. Hendry, F. Wang, J. Shan, T. F. Heinz and M. Bonn, *Phys. Rev. B*, 2004, **69**, 081101.

4 N. A. Deskins and M. Dupuis, *Phys. Rev. B*, 2007, **75**, 195212.

5 G. Mattioli, P. Alippi, F. Filippone, R. Caminiti and A. Amore Bonapasta, *J. Phys. Chem. C*, 2010, **114**, 21694–21704.

6 A. Janotti, C. Franchini, J. B. Varley, G. Kresse and C. G. Van de Walle, *Phys. Status Solidi RRL*, 2013, **7**, 199–203.

7 P. Deák, B. Aradi and T. Frauenheim, *Phys. Rev. B*, 2011, **83**, 155207.

8 D. Bi, W. Tress, M. I. Dar, P. Gao, J. Luo, C. Renevier, K. Schenk, A. Abate, F. Giordano, J.-P. Correa Baena, J.-D. Decoppet, S. M. Zakeeruddin, M. K. Nazeeruddin, M. Gratzel and A. Hagfeldt, *Sci. Adv.*, 2016, **2**, 1501170.

9 M. Sachs, E. Pastor, A. Kafizas and J. R. Durrant, *J. Phys. Chem. Lett.*, 2016, 3742–3746.

10 Y. Yamada and Y. Kanemitsu, *Phys. Rev. B*, 2010, **82**, 113103.

11 Y. Tezuka, S. Shin, A. Agui, M. Fujisawa and T. Ishii, *J. Phys. Soc. Jpn.*, 1996, 65, 312–317.

12 A. Fujishima, X. ZHANG and D. A. Tryk, *Surf. Sci. Rep.*, 2008, **63**, 515–582.

13 A. Argondizzo, X. Cui, C. Wang, H. Sun, H. Shang, J. Zhao and H. Petek, *Phys. Rev. B*, 2015, **91**, 155429.

14 Z. Wang, B. Wen, Q. Hao, L.-M. Liu, C. Zhou, X. Mao, X. Lang, W.-J. Yin, D. Dai, A. Selloni and X. Yang, *J. Am. Chem. Soc.*, 2015, **137**, 9146–9152.

15 Y. Zhang, D. T. Payne, C. L. Pang, H. H. Fielding and G. Thornton, *J. Phys. Chem. Lett.*, 2015, **6**, 3391–3395.

16 F. Frassetto, C. Cacho, C. A. Froud, I. C. E. Turcu, P. Villoresi, W. A. Bryan, E. Springate and L. Poletto, *Opt. Express*, 2011, **19**, 19169–81.

17 C. M. Yim, C. L. Pang and G. Thornton, *Phys. Rev. Lett.*, 2010, **104**, 036806.

18 A. C. Papageorgiou, N. S. Beglitis, C. L. Pang, G. Teobaldi, G. Cabailh, Q. Chen, A. J. Fisher, W. a Hofer and G. Thornton, *Proc. Natl. Acad. Sci. U. S. A.*, 2010, **107**, 2391–2396.

19 C. L. Pang, R. Lindsay and G. Thornton, *Chem. Soc. Rev.*, 2008, **37**, 2328–2353.

20 L. Miaja-Avila, C. Lei, M. Aeschlimann, J. L. Gland, M. M. Murnane, H. C. Kapteyn and G. Saathoff, *Phys. Rev. Lett.*, 2006, **97**, 113604.

21 V. M. Khomenko, K. Langer, H. Rager and A. Fett, *Phys. Chem. Miner.*, 1998, **25**, 338–346.

22 K. Vos, *J. Phys. C Solid State Phys.*, 1977, **10**, 3917.

23 L. Chiodo, J. M. García-Lastra, A. Iacomino, S. Ossicini, J. Zhao, H. Petek and A. Rubio, *Phys. Rev. B*, 2010, **82**, 045207.

24 L. Kronik and Y. Shapira, *Surf. Sci. Rep.*, 1999, **37**, 1–206.

25 K. Ozawa, M. Emori, S. Yamamoto, R. Yukawa, S. Yamamoto, R. Hobara, K. Fujikawa, H. Sakama and I. Matsuda, *J. Phys. Chem. Lett.*, 2014, **5**, 1953–1957.

26 K. Onda, B. Li, J. Zhao, K. D. Jordan, J. L. Yang and H. Petek, *Science*, 2005, **308**, 1154–1158.

27 V. P. Zhukov and E. V Chulkov, *J. Phys. Condens. Matter*, 2010, **22**, 435802.

28 L. Gundlach, R. Ernstorfer and F. Willig, *Prog. Surf. Sci.*, 2007, **82**, 355–377.

29 D. M. M. Eagles, *J. Phys. Chem. Solids*, 1964, **25**, 1243–1251.

30 J. G. Traylor, H. G. Smith, R. M. Nicklow and M. K. Wilkinson, *Phys. Rev. B*, 1971, **3**,

3457–3472.

31 S. Moser, S. Fatale, P. Krüger, H. Berger, P. Bugnon, A. Magrez, H. Niwa, J. Miyawaki, Y. Harada and M. Grioni, *Phys. Rev. Lett.*, 2015, **115**, 096404.

32 R. J. Ellingson, J. B. Asbury, S. Ferrere, H. N. Ghosh, J. R. Sprague, T. Lian and A. J. Nozik, *J. Phys. Chem. B*, 1998, **102**, 6455–6458.

33 A. Kazempour, *Phys. Scr.*, 2015, **90**, 025804.

34 J. J. Yeh and I. Lindau, *At. Data Nucl. Data Tables*, 1985, **32**, 1.

35 M. Xu, Y. Gao, E. M. Moreno, M. Kunst, M. Muhler, Y. Wang, H. Idriss and C. Wöll, *Phys. Rev. Lett.*, 2011, **106**, 138302.

36 Y. Yamada and Y. Kanemitsu, *Appl. Phys. Lett.*, 2012, **101**, 133907.

37 L. Zhang, Q. Zheng, Y. Xie, Z. Lan, O. V. Prezhdo, W. A. Saidi and J. Zhao, *Nano Lett.*, 2018, **18**, 1592–1599.

38 W. Shockley and W. T. Read, *Phys. Rev.*, 1952, **87**, 835–842.

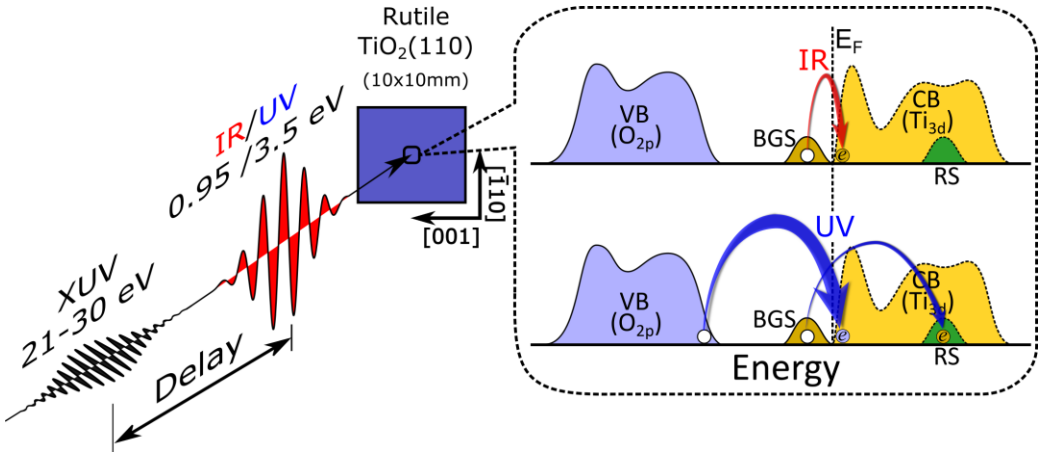

Fig. 1. Scattering geometry of the pump probe experiments, with light incident at 45˚ in the [001] azimuth. The pump electric field of the incident light is parallel to the [$\bar{1}$10] azimuth. The dashed box shows the excitation routes for IR and UV pumped experiments. IR can excite electrons from the band gap states (BGS) to the bottom of the conduction band (CB), while UV can excite electrons both from the BGS to a resonance state (RS) in the conduction band (small arrow) and from the valence band (VB) to the conduction band (large arrow).

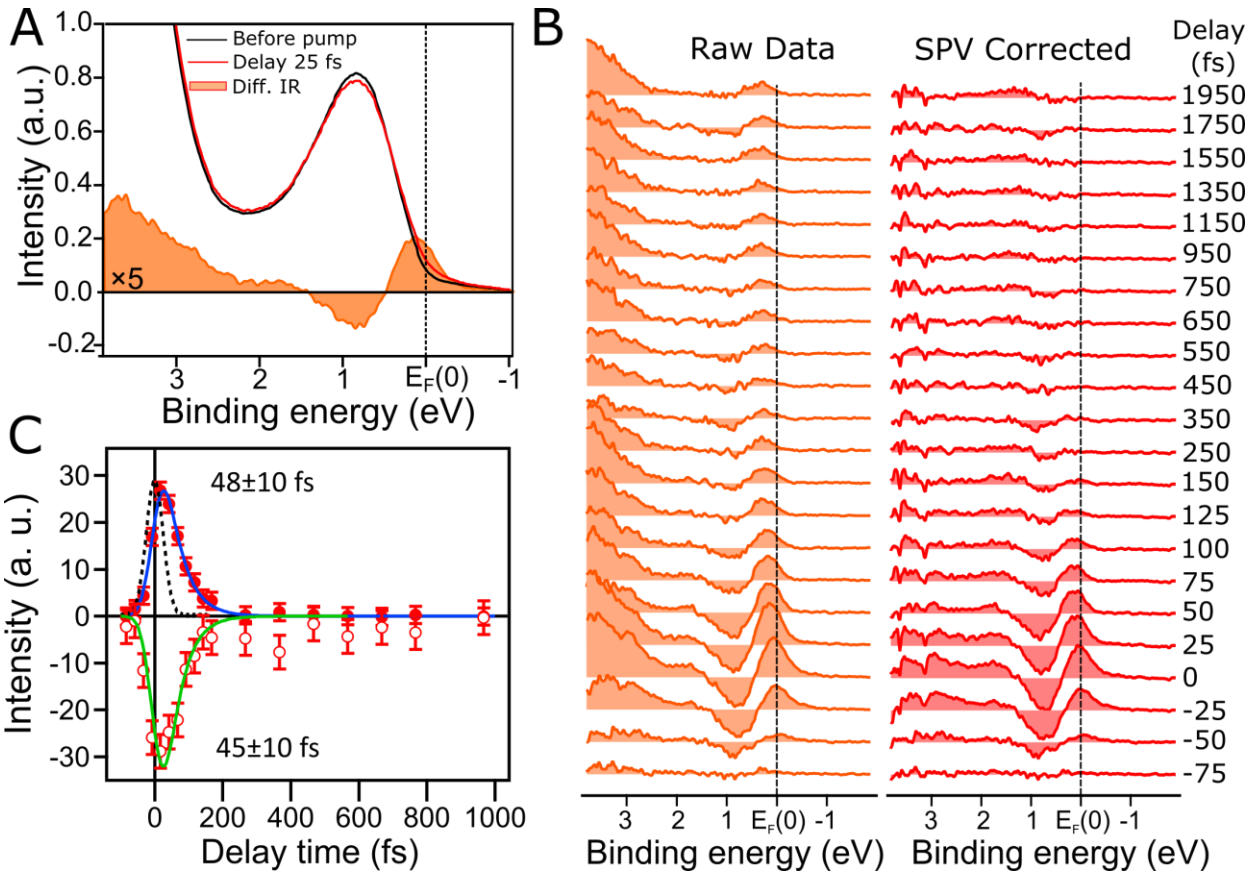

Fig. 2. **A** Photoemission spectra (hν = 20.9 eV) before the IR pump pulse (black) and at a delay time of 25 fs (red). The difference between the two spectra is shown as the filled spectrum. **B** The difference spectra measured at different delay times. Left panel shows the raw data. The difference spectra after the correction for the SPV effect (shifting the delayed spectra by about 10 meV) are shown on the right. **C** The evolution of hot electrons (filled circles) at E_F and recovery of the BGS peak (open circles) as a function of delay time. The intensities are obtained from the difference within an energy window of 0.3 eV centred at 0 eV binding energy (hot electrons around E_F) and 0.9 eV (band gap state) binding energy, respectively. A single exponential decay function convolved with the cross correlation function (black dashed curve) is employed to fit the data.

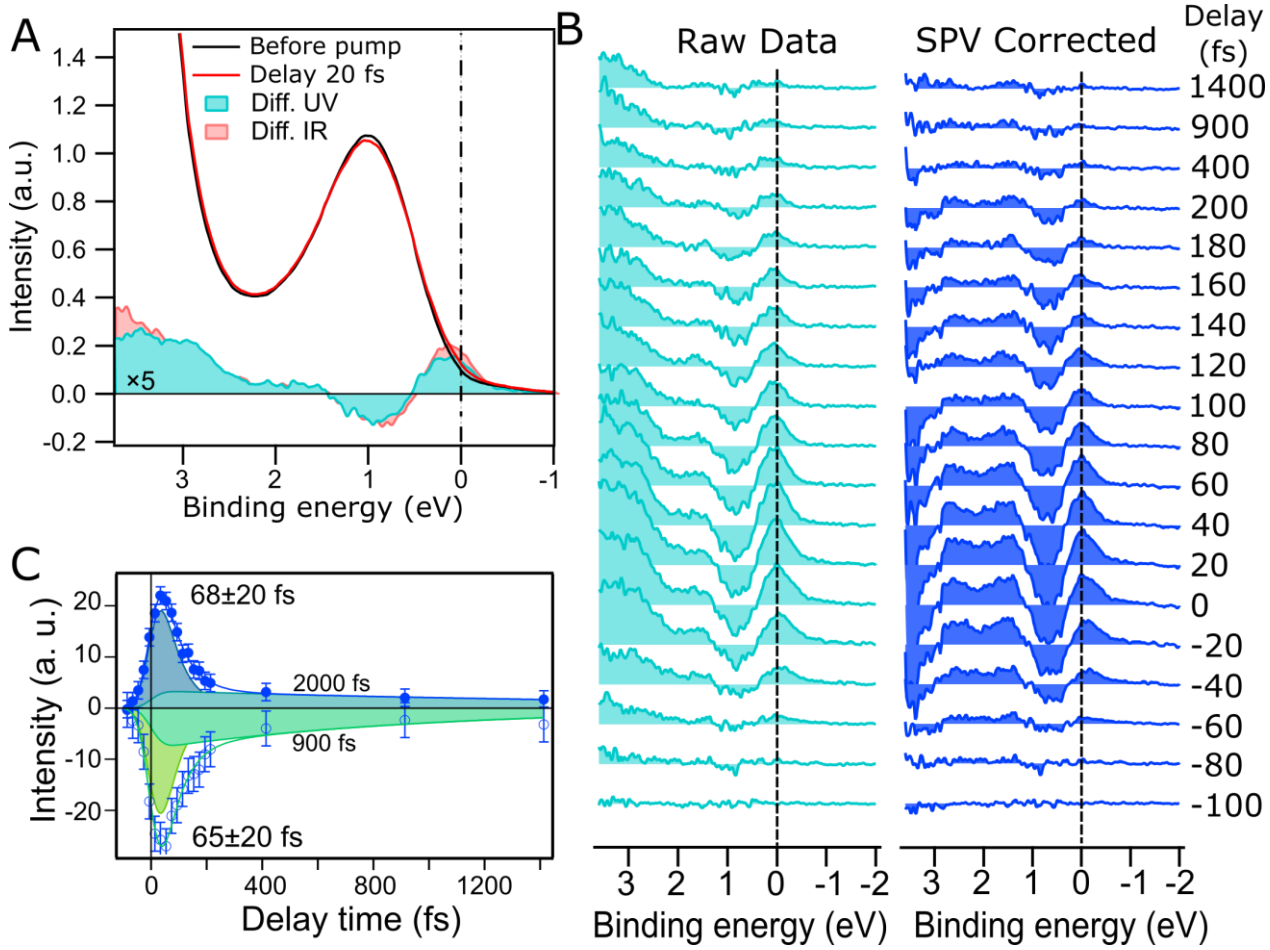

Fig. 3. **A** Photoemission spectra (hν = 30.4 eV) before the UV pump pulse (black) and at a delay time of 20 fs (red). The difference between the two spectra is shown as the filled spectrum. As a comparison, the difference from the IR pumped experiments (delay time 25 fs) is also shown. **B** The difference spectra measured at different delay times. Left panel shows the raw data. The difference spectra after the correction for the SPV effect (shifting the delayed spectra by about 10 meV) are shown on the right. **C** The evolution of hot electrons at E_F and recovery of the BGS peak as a function of delay time. The intensities are obtained from the difference spectra within an energy window of 0.3 eV centred at 0.9 eV binding energy (open circles) and 0 eV (filled circles) binding energy, respectively. Two exponential decay functions convolved with the cross correlation function are used to fit the data.

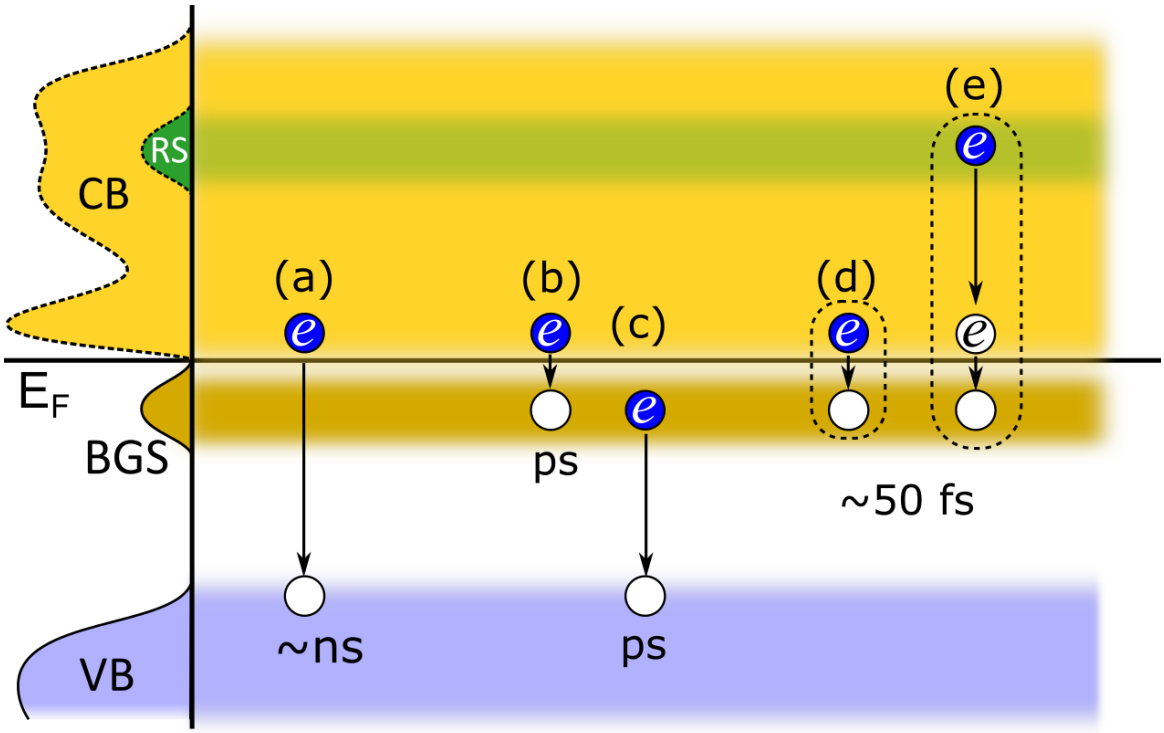

Fig. 4. Recombination processes on TiO_2 in order of increasing recombination rate: (a) Direct recombination of band electrons and holes created by band gap excitation; (b) trapping of band electrons created by band gap excitation as polarons; (c) recombination of BGS electrons with valence band holes created by band gap excitation; (d) localised electrons excited from the BGS are retrapped as polarons; (e) similar to (d) but the electrons are first excited from the BGS to the resonance state (RS) in the conduction band, then decay rapidly to lower energies and are finally trapped as polarons. The approximate lifetimes are indicated. The dashed boxes indicate the localised nature of the transitions.